Biofuels and Environmental Biotechnology **Biotechnology and Bioengineering**
DOI 10.1002/bit.26021

Optimization of an acetate reduction pathway for producing cellulosic ethanol by engineered yeast†

Guo-Chang Zhang[a,b,1], In Iok Kong[a,b,1], Na Wei[c], Dairong Peng[b], Timothy L Turner[b], Bong Hyun Sung[d], Jung-Hoon Sohn[d], Yong-Su Jin[a,b,*]

Running title: Optimization of the acetate reduction pathway in yeast

[a] Carl R. Woese Institute for Genomic Biology, University of Illinois at Urbana-Champaign, Urbana, IL 61801, USA.
[b] Department of Food Science and Human Nutrition, University of Illinois at Urbana-Champaign, Urbana, IL 61801, USA.
[c] Department of Civil and Environmental Engineering and Earth Sciences, University of Notre Dame, South Bend, IN, 46556, USA.
[d] Bioenergy and Biochemical Research Center, Korea Research Institute of Bioscience and Biotechnology, 125 Gwahak-ro, Yuseong-gu, Daejeon 34141, Korea

[1] The two authors contributed equally to this work.

* Corresponding author: Yong-Su Jin (ysjin@illinois.edu).
Mailing address: 1206 W. Gregory Dr., Institute for Genomic Biology, Urbana, IL, 61801, United States.

†This article has been accepted for publication and undergone full peer review but has not been through the copyediting, typesetting, pagination and proofreading process, which may lead to differences between this version and the Version of Record. Please cite this article as doi: [10.1002/bit.26021]

Additional Supporting Information may be found in the online version of this article.

Received April 6, 2016; Revision Received May 24, 2016; Accepted May 27, 2016

Abstract

Xylose fermentation by engineered *Saccharomyces cerevisiae* expressing NADPH-linked xylose reductase (XR) and NAD^+-linked xylitol dehydrogenase (XDH) suffers from redox imbalance due to cofactor difference between XR and XDH, especially under anaerobic conditions. We have demonstrated that coupling of an NADH-dependent acetate reduction pathway with surplus NADH producing xylose metabolism enabled not only efficient xylose fermentation, but also *in situ* detoxification of acetate in cellulosic hydrolysates through simultaneous co-utilization of xylose and acetate. In this study, we report the highest ethanol yield from xylose (0.463 g ethanol/g xylose) by engineered yeast with XR and XDH through optimization of the acetate reduction pathway. Specifically, we constructed engineered yeast strains exhibiting various levels of the acetylating acetaldehyde dehydrogenase (AADH) and acetyl-CoA synthetase (ACS) activities. Engineered strains exhibiting higher activities of AADH and ACS consumed more acetate and produced more ethanol from a mixture of 20 g/L of glucose, 80 g/L of xylose, and 8 g/L of acetate. In addition, we performed environmental and genetic perturbations to further improve the acetate consumption. Glucose-pulse feeding to continuously provide ATPs under anaerobic conditions did not affect acetate consumption. Promoter truncation of *GPD1* and gene deletion of *GPD2* coding for glycerol-3-phosphate dehydrogenase to produce surplus NADH also did not lead to improved acetate consumption. When a cellulosic hydrolysate was used, the optimized yeast strain (SR8A6S3) produced 18.4% more ethanol and 41.3% less glycerol and xylitol with consumption of 4.1 g/L of acetate than a control strain without the acetate reduction pathway. These results suggest that the major limiting factor for enhanced acetate reduction during the xylose fermentation might be the low activities of AADH and ACS, and that the redox imbalance problem of XR/XDH pathway can be exploited for *in situ* detoxification of acetic acid in cellulosic hydrolysate and increasing ethanol productivity and yield.

Keywords: *Saccharomyces cerevisiae*; Xylose; Acetate; Co-consumption; *adhE*; Acetyl-coA synthetase.

1. Introduction

*Saccharomyces cerevisia*e, which has been widely used for first generation biofuel, cannot naturally utilize xylose which is abundant in cellulosic hydrolysates (Jeffries and Jin 2004; Wei et al. 2013; Zhang et al. 2015). As such, metabolic engineering approaches to develop rapid and efficient xylose-consuming engineered *S. cerevisiae* have been undertaken for decades (Ho et al. 1998; Kim et al. 2013; Kuyper et al. 2005; Zhou et al. 2012). Numerous xylose-fermenting *S. cerevisiae* strains have been constructed, with either a cofactor-dependent xylose reductase (XR)-xylitol dehydrogenase (XDH) pathway or a cofactor-independent xylose isomerase (XI) pathway. Whereas the engineered *S. cerevisiae* strains with the XR-XDH pathway are advantageous in terms of ethanol productivity, the engineered strains with XI pathway are better in terms of ethanol yield (Karhumaa et al. 2007; Li et al. 2016).

In addition to xylose fermentation issue, the toxicity of acetic acid, which is generated by hydrolysis of acetyl groups in hemicellulose (Palmqvist and Hahn-Hägerdal 2000b), is another outstanding problem for producing cellulosic ethanol. Acetate severely hinders both yeast growth and intracellular sugar metabolism (Axe and Bailey 1995; Jonsson et al. 2013; Klinke et al. 2004; Palmqvist and Hahn-Hägerdal 2000a; Palmqvist and Hahn-Hägerdal 2000b). Previous studies have focused on identifying gene targets eliciting improved tolerance against acetate (Chen et al. 2016; Haitani et al. 2012; Kawahata et al. 2006; Tanaka et al. 2012). *AFT1* and *HAA1* coding for two transcription factors involved in iron utilization and weak acid stress adaptation, respectively, have been reported to be up-regulated in the presence of acetate. Genetic perturbations of *AFT1* and *HAA1* led to marginal improvements in acetate tolerance, but acetate remained in the fermentation medium without detoxification.

While native *S. cerevisiae* can consume acetate as a carbon source through respiratory metabolism using molecular oxygen as an electron acceptor (Burtner et al. 2009; Wang et al. 1952), this yeast cannot consume acetate under anaerobic conditions. A possible anaerobic route of acetate consumption

is to convert acetate into acetyl-CoA by acetate synthetase and then reduce acetyl-CoA into ethanol by acetylating acetaldehyde dehydrogenase (AADH) (Atteia et al. 2003; Fontaine et al. 2002; Wei et al. 2013). *S. cerevisiae* lacks AADH so that introduction of a heterologous gene coding for AADH into *S. cerevisiae* is necessary to reduce acetate. The possibility of using acetate as an electron acceptor to eliminate glycerol production in yeast during glucose fermentation has been demonstrated (Guadalupe Medina et al. 2010). However, the two genes encoding NAD-dependent glycerol-3-phosphate dehydrogenase (*GPD1* and *GPD2*) need to be deleted to build up surplus NADH accumulation which could serve as reducing power for acetic acid reduction, causing severe growth defect of the engineered yeast.

In contrast to glucose metabolism, xylose metabolism by XR and XDH generates surplus NADH due to cofactor differences of NADPH-linked XR and NAD^+-linked XDH. Surplus NADH produced during xylose fermentation has been pointed out as a problem causing the accumulation of reduced byproducts (xylitol and glycerol). However, the surplus NADH from xylose fermentation can be exploited for detoxifying acetate into ethanol through introducing AADH (coded by *E. coli adhE* gene) into a xylose-fermenting engineered *S. cerevisiae* (Wei et al. 2013). This strategy can provide multiple benefits for producing cellulosic ethanol. First, it allows *in situ* detoxification of acetate from lignocellulosic hydrolysates. Second, ethanol yield can increase as acetate is converted into ethanol. Third, byproducts formation such as xylitol and glycerol can be reduced as surplus NADH is exploited to acetate reduction. Nonetheless, only small fractions (~10-15%) of acetate in the cellulosic hydrolysates have been consumed into ethanol (Wei et al. 2015; Wei et al. 2013).

In this study, we optimized the acetate reduction pathway for the enhanced conversion of acetate into ethanol during xylose fermentation. As the theoretical maximum ethanol yield from acetate (0.77 g ethanol/g acetate) is much higher than that (0.51 g ethanol/g xylose) from xylose, complete conversion of 15 g/L of acetate (typical concentrations of acetate in cellulosic hydrolysates) into ethanol might produce the amount of ethanol which can be produced from 23 g/L of xylose, suggesting a great

potential of the acetate reduction pathway to reduce the cost of cellulosic ethanol. Through optimizing the expression levels of AADH and ACS in the acetate reduction pathway, we have made substantial improvements in actual lignocellulosic hydrolysates. The optimized engineered strain SR8A6S3 exhibited ethanol yield up to 0.463 g/g xylose under anaerobic condition, which is so far the closest to the theoretical maximum ethanol yield from sugars by engineered yeast strains with XR and XDH pathway.

2. Materials and methods

2.1. Strains, media and growth conditions.

Escherichia coli Top10 was used for the construction and routine preparation of plasmids used in this study. *E. coli* was grown in LB medium (5 g/L yeast extract, 10 g/L tryptone, 10 g/L NaCl, pH 7.0) at 37 °C, and ampicillin (100 μg/mL) was added when required. The yeast strain used in this study was *S. cerevisiae* SR8 (Kim et al. 2013) which is an efficient xylose-utilizing yeast. For fermentation experiments, yeast strains were grown in yeast extract-peptone (YP) medium (10 g/L yeast extract, 20 g/L peptone) containing glucose (YPD), xylose (YPX), acetate (YPA) or a mixture of glucose, xylose, and acetate (YPDXA). Lignocellulosic hydrolysates from National Renewable Energy Laboratory (NREL) were also used for fermentation experiments. The concentrations of the sugars were placed as numbers following their initials (e.g., YPD20 represents YP medium containing 20 g/L glucose; YPD20X80A8 represents YP medium containing 20 g/L glucose, 80 g/L xylose, and 8 g/L acetic acid). Defined minimal medium (YSCD) containing 6.7 g/L yeast nitrogen base without amino acids and supplemented with the appropriate auxotrophic requirements and 20 g/L glucose was used for routine yeast transformations. All yeast experiments were performed at 30 °C.

2.2. Plasmid and strain construction.

The open reading frame (ORF) of *E. coli adhE* gene (Wei et al. 2013) was codon-optimized based

on codon usages of the genes coding for highly expressed glycolytic enzymes in yeast (Wiedemann and Boles 2008) and synthesized by IDT Inc., USA. Two integration plasmids YIplac211 (Gietz and Sugino 1988) and pITy3 (Parekh et al. 1996) were used as backbones to construct the wild-type and codon-optimized *adhE* overexpression cassettes. The plasmid YIplac211-H1H2 (Table 2) was constructed by ligating two adjacent DNA fragments H1 (digested by EcoRI and KpnI) and H2 (digested by HindIII and SphI) from a yeast intergenic region into YIplac211 sequentially. The fragments H1 and H2, used as homology arms for double-crossover integration, were PCR amplified using primer pairs H1-U/H1-D and H2-U/H2-D (Table 1). The yeast constitutive promoter pPGK1 and its terminator tPGK1 were PCR amplified using primer pairs listed in Table 1 and then ligated into plasmid pITy3. The wild-type *adhE* gene (WT_*adhE*) and codon-optimized *adhE* gene (CO_*adhE*) were inserted in between of the pPGK1 and tPGK1, forming plasmid pITy3-pPGK1-WT*adhE*-tPGK1 and pITY3-pPGK1-CO*adhE*-tPGK1. The WT_*adhE* and CO_*adhE* overexpression cassettes were then PCR amplified by primer pair adhE-U and adhE-D (Table 1) and then ligated into plasmid YIplac211-H1H2 between fragments H1 and H2, respectively, forming plasmid YIplac211-H1H2-WT_*adhE* and YIplac211-H1H2-CO_*adhE*.

YIplac211-H1H2-WT_*adhE* and YIplac211-H1H2-CO_*adhE* were then linearized by restriction enzyme *Spe*I and transformed into SR8 strain, respectively. After transformation, cells were plated on selective media (SCD-ura plate) and allowed to grow for 2-3 days until colonies were ready to pick. Colonies with the successful integration of genes were confirmed by diagnostic PCR, and the resulted strains designated as SR8A2 and SR8A4 (Table 3), respectively. Plasmid pITy3-pPGK1-CO_*adhE*-tPGK1 was linearized by restriction enzyme *Xho*I and transformed into the SR8A4 strain. Transformants were selected on YPD plate supplemented with an appropriate amount of Hygromycin B. The resulted strain was designated as SR8A5 (Table 3). One more copy of CO_*adhE* was integrated into the SR8A5 strain at the mutated *PHO13* (Kim et al., 2013) locus using a CRISPR-Cas9 based metabolic engineering tool (DiCarlo et al. 2013; Zhang et al. 2014). The guide RNA (gRNA) plasmid

gRNA-pho13-G418 for targeting the mutant *PHO13* locus was constructed using the method as previously described (Zhang et al. 2014). Cas9-NAT was transformed into the SR8A5 strain to obtain the SR8A5-Cas9 strain selected on a YPD plate supplemented with an appropriate amount of ClonNAT (Nourseothricin, a streptothricin antibiotic). A long double strand donor DNA containing CO_*adhE* overexpression cassette flanked by 60 bp homology arms was PCR amplified from plasmid YIplac211-H1H2-CO_*adhE* using primer pair adhEdonor-U and adhEdonor-D (Table 1). The resulting linear expression cassette was transformed together with plasmid gRNA-pho13-G418 into the SR8A5-Cas9 strain. The transformants were selected on YPD plate supplemented with 120 mg/mL ClonNAT and 300 mg/mL G418 afterward. Positive colonies were confirmed by diagnostic PCR and designated as the SR8A6 strain.

The mutant *Salmonella ACS* gene overexpression plasmid ACS*Opt was a kind gift from Dr. Huimin Zhao (Lian et al. 2014). The overexpression of this mutated *ACS* was achieved by a CRISPR-Cas9 based integration method as mentioned above. Three copies of *ACS* overexpression cassette were integrated into the SR8A6 strain iteratively at three different intergenic loci. The final resulting strain was designated as the SR8A6S3 strain.

SR8A5-1, SR8A5-2, SR8A5-3 AND SR8A5-4 strains were derived from the SR8A5 strain for manipulating intracellular NADH level according to previous literature (Ding et al. 2013). The SR8A5-1 strain was generated by introducing 60 bp *GPD1* promoter truncation in the SR8A5 strain. The SR8A5-2 strain was obtained by introducing 80 bp *GPD1* promoter truncation in the SR8A5 strain. The SR8A5-3 was made by deleting *GPD2* in the SR8A5-1 strain. The SR8A5-4 was constructed by deleting *GPD2* in the SR8A5-2 strain. All the deletions and promoter truncations were achieved by using a CRISPR-Cas9 based method.

2.3. Crude extract preparation for enzymatic assays.

We followed the protein extraction procedure reported previously with slight modifications

(Vickers et al. 2013). To prepare the protein extract, overnight pre-cultures were inoculated into 20 mL YP with 20 g/L glucose, 40 g/L xylose, and 2 g/L acetate and fermented anaerobically till the OD_{600} reached 1 or 2. Yeast cells were then harvested and centrifuged at 4,000 rpm and 4 °C for 5 min. Cell pellets were washed twice with cold H_2O, and then resuspended in 1 mL of cocktail mix that contains a 50 mL mixture of a protease inhibitor cocktail tablet (Roche Applied Science, Indianapolis, IN), 25 mM Tris-HCl pH 7.5, and 1 mM dithiothreitol. The cell suspension was transferred into chilled 2 mL tubes filled with acid-washed glass beads (Ø = 0.5 mm). Yeast cells were disrupted with FastPrep ® Cell Disrupter (MP Biomedicals, Santa ana, CA). Ruptured cells were centrifuged at 18,000 rpm for 10 min at 4 °C, and the supernatant was used as the protein extract. Protein concentration was determined by Thermo Scientific Pierce BCA Protein Assay Kit (Thermo Fisher Scientific, Waltham, MA) as described by the supplier.

2.4. Enzymatic activity assays.

AADH enzymatic reaction was initiated by adding 5 µL of a crude extract and 1.2 mM acetyl coenzyme into the mixture of 0.3 mM NADH in 50 mM potassium phosphate buffer (pH 7.5) with a total reaction volume of 200 µL (Wei et al. 2013). The enzyme activities were measured by detecting the oxidation of NADH from the absorbance changes at 340 nm at 30 °C using BioTek's Synergy HT plate reader (Biotek, Winooski, VT). Specific activities are expressed as units per milligram of protein. Units are defined as micromoles of NADH reduced or oxidized per minute. All samples were analyzed in triplicates experiments.

ACS enzyme activity was measured by coupled reactions of malate dehydrogenase and citrate synthase (van den Berg et al. 1996) with a net reaction of acetate + ATP + L-malate + NAD^+ → citrate + AMP + NADH. The enzymatic reaction was initiated by adding 20 µL of 1 M sodium acetate and 40 µL of a crude extract into the mixture (140 µL) with final concentrations of 35 mM Tris-HCl (pH 7.8), 2.5 mM L-malate, 1 mM ATP, 2.5 mM $MgCl_2$, 0.1 mM coenzyme A trilithium salt, 3 mM NAD^+, 2.5

units of malate dehydrogenase, and 1.25 units of citrate synthase. ACS enzymatic activities were measured by formation of NADH (reduction of NAD^+). Specific activities are expressed as units per milligram of protein. Units are defined as micromoles of NADH produced per minute.

2.5. Fermentation and metabolite analysis.

"Pretreated *Miscanthus* biomass " was generated in a National Renewable Energy Lab (NREL), Golden, CO, pretreatment pilot plant and 25% (w/w) solid loading, 1.5% (w/w) sulfuric acid and a rapid steam-driven heating ramp to 190°C with a holding time of 1 min and subsequent rapid pressure release/cooling. The liquid fraction of *Miscanthus* hydrolysate was neutralized to pH 6.5 with calcium hydroxide. In order to supplement nitrogen sources and necessary nutrient for yeast growth, 0.1X YP medium (1 g/L yeast extract and 2 g/L peptone) was supplemented. The resulting hydrolysate contained approximately 20 g/L glucose, 50 g/L xylose, 10 g/L acetate, 1 g/L HMF, and 2 g/L furfural. Anaerobic batch fermentation experiments were performed by inoculating yeast cells grown on YPD into 10 mL fermentation media (YP medium containing 20 g/L glucose, 80 g/L xylose, and 8 g/L acetate, or above-mentioned lignocellulosic hydrolysates). Initial cell densities were OD600 of ~1 (corresponding to approximately 0.24 g/L dry cell mass) for YP medium and ~10 (corresponding to approximately 2.4 g/L dry cell mass) for lignocellulosic hydrolysates. A serum bottle sealed with butyl rubber stoppers was used to ensure strict anaerobic conditions. The serum bottles with fermentation media were then flushed with nitrogen gas, which had passed through a heated, reduced copper column to remove trace of oxygen. Fermentations were performed at 30 °C and 100 rpm conditions. Samples were taken at appropriate intervals and then centrifuged at 15,000 rpm for 5 min. Supernatants were diluted appropriately and then used for the determination of glucose, xylose, glycerol, acetic acid and ethanol by high-performance liquid chromatography (HPLC, Agilent Technologies 1200 Series) equipped with a refractive index detector. The Rezex ROA-Organic Acid H+ (8%) column (Phenomenex Inc., Torrance, CA) was used and the columns were eluted with 0.005 N H_2SO_4 at 50 °C, and the flow rate

was set at 0.6 mL/min.

3. Results

3.1. Construction of engineered yeast strains exhibiting different AADH and ACS activities.

AADH and ACS are the two key enzymes of the acetate reduction pathway (Figure 1). We hypothesized that enhanced activities of the two enzymes might increase the rate of acetate consumption in engineered yeast. Thus, we constructed a series of engineered strains exhibiting varied levels of AADH and ACS activities. We attempted to increase AADH activity gradually through codon-optimization and increasing copy numbers of the expression cassette containing codon optimized *adhE* (CO_*adhE*) under the control of the PGK promoter (P_{PGK}) (Figure 2A). The starting strain SR8 as a control showed almost no AADH activity but the SR8A2 strain harboring one copy of the expression cassette expressing the wild-type *adhE* showed measurable levels of AADH activities (1.77 folds higher than basal activity given by control SR8 strain). In order to increase the AADH activity in our engineered yeast, we introduced an expression cassette containing codon-optimized *adhE* into the SR8 strain. The resulting SR8A4 showed a three-fold higher AADH activity than the SR8A2 strain, suggesting that the codon-optimized *adhE* (CO_*adhE*) is expressed much better than the wild-type *adhE* (WT_*adhE*) in *S. cerevisiae*. By iteratively introducing the expression cassette containing CO_*adhE* into the SR8A4 strain, the SR8A5 strain containing two copies of CO_*adhE* and the SR8A6 strains containing three copies of CO_*adhE* were constructed. As a result, four engineered strains (SR8A2, SR8A4, SR8A5, and SR8A6) exhibiting various levels of AADH activity were constructed (Figure 2A).

To enhance ACS activity, we chose to overexpress a mutant ACS from *Salmonellas enterica* which was reported to have less feedback regulation by acetyl-CoA (Lian et al. 2014; Shiba et al. 2007). We reasoned that the increased activity by the mutant ACS could facilitate enhanced utilization of acetate. As such, we introduced three copies of the expression cassette containing this mutant ACS into the

SR8A6 strains. The resulting SR8A6S3 strain showed two-fold higher ACS activity than other engineered yeast strains (Figure 2B). These results suggest that with the combination of codon optimization and augmentation of copy number, the activities of the two key enzymes AADH and ACS can be substantially elevated in engineered yeast strains.

3.2. Improved acetate consumption under anaerobic conditions by the engineered yeast strains.

We carried out anaerobic fermentation to evaluate the acetate consumption capacities of our engineered strains with varied AADH and ACS activities (SR8A2, SR8A4, SR8A5, SR8A6, and SR8A6S3 using SR8 as a control). In order to mimic the fermentation of lignocellulosic hydrolysates, 20 g/L glucose, 80 g/L xylose, and 8 g/L of acetic acid were supplemented in the YP medium as carbon sources. As expected, the engineered yeast strains with higher AADH and ACS activities consumed more acetate and produced less reduced byproducts (glycerol and xylitol) when they finished xylose fermentation, resulting in producing more ethanol. Moreover, we observed a positive correlation between AADH/ACS activities and the amounts of consumed acetate (Figure 3A, Figure S1F). Similar to control SR8 strain, the SR8A2 strain expressing *E. coli adhE* (WT_*adhE*) consumed only little amounts of acetate (Figure 2A) but the SR8A4 strain expressing a codon optimized *adhE* (CO_*adhE*) showed much better acetate consumption of up to 3.28 g/L, suggesting that *E. coli adhE* (WT_*adhE*) might be expressed poorly in yeast. The SR8A5 strain containing an extra copy of the expression cassette of CO_*adhE* was able to consume 5.28 g/L of acetate but the SR8A6 strain containing two extra copies of the expression cassette of CO_*adhE* consumed almost same amounts of acetate even though the SR8A6 strain had a higher AADH activity than the SR8A5 strain (Figure 2A). This result suggests that there might be a saturation of AADH activity for acetate consumption in the SR8A6 strain.

Nevertheless, we decided to use the SR8A6 strain for introducing a mutant ACS as the saturation might be relieved when ACS activity increases. As such, we introduced three copies of the mutant ACS into the genome of the SR8A6 strain. The resulting strain SR8A6S3 consumed 7.1 g/L of acetate. As a

result, the SR8A6S3 strain produced the least amounts of the reduced byproducts (2.5 g glycerol/L and 1.84 g xylitol/L) and the most amount of ethanol (43.33 g ethanol/L), while the control SR8 strain produced the most amounts of reduced byproducts (8.24 g glycerol/L and 5.72 g xylitol/L) and the least amount of ethanol (30.39 g ethanol/L). The ethanol titer of the SR8A6S3 strain exhibited a significant increase of 42.6% as compare to the control SR8 strain.

The ethanol yields of the engineered yeast strains with varied AADH and ACS activities gradually increased 29.7% from 0.344 g ethanol/g sugars to 0.446 g ethanol/g sugars (Figure 3B, Figure 5A, and Figure 5B) (Table 4). Glycerol and xylitol yield gradually decreased because the redox imbalance in the engineered strains can be alleviated stepwise as more acetate consumed. Specifically, the glycerol yields of the engineered strains decreased 69.7% from 0.089 g glycerol/g sugar to 0.027 g glycerol/g sugars (Figure 3C, Figure 5A, and Figure 5B) (Table 4) and the xylitol yields decreased 71.8% from 0.085 g xylitol/g xylose to 0.024 g xylitol/g xylose (Figure 3D, Figure 5A, and Figure 5B) (Table 4). The acetate reduction pathway in the SR8A6S3 contributed a 70.7% lower byproduct yield and 29.7% higher ethanol yield as compared to the control SR8 strain. These results suggest that the acetate consumption capacity can be improved by increasing the activities of AADH and ACS.

3.3. Effects of glucose pulse-feeding on acetate consumption

The acetate reduction pathway is coupled with ATP consumption (Figure 1). ACS which is the first enzyme in the pathway uses 2 ATP equivalents. Therefore, we reasoned that the metabolic fluxes towards the acetate reduction pathway could be limited if intracellular ATP levels are not sufficient to support the ACS reaction even though the activities of ACS and AADH increased. In order to examine whether or not the elevated ATP levels could positively affect acetate consumption, we conducted a glucose pulse-feeding fermentation to supplement ATP in a continuous manner as the substrate-level phosphorylation is the only way for generating ATP. The SR8A6S3 strain was chosen as it exhibited highest activities of both ACS and AADH. While we used the same amounts of glucose (20 g/L),

xylose (80 g/L), and acetic acid (8 g/L) for the fermentation experiment, we started the fermentation with 6 g/L of initial glucose, 80 g/L of xylose, and 8 g/L of acetate and the rest of glucose (14 g/L) was pulse-fed to the culture every 12 hours instead of providing 20 g/L of glucose initially. As is shown in Figure S2, the consumption of acetate during the pulse-feeding fermentation was almost identical to the previous batch fermentation under the same conditions, suggesting that continuous ATP generation by glucose pulse-feeding could not assist the acetate reduction pathway.

3.4. Effects of altered glycerol-3-phosphate dehydrogenase expression levels on acetate consumption.

In addition to ATP for ACS, AADH requires NADH as a cofactor. As surplus NADH is produced during anaerobic xylose fermentation in engineered yeast strain with XR-XDH pathway (Jeffries and Jin 2004), it is possible to couple the surplus NADH with the acetate reduction pathway (Wei et al. 2013). However, we cannot exclude the possibility that NADH levels under this circumstance are still limiting. In order to examine if the acetate consumption capacity of the engineered strains can be affected by elevated NADH levels, four engineered yeast strains (SR8A5-1, SR8A5-2, SR8A5-3 and SR8A5-4) exhibiting different expression levels of NAD-dependent glycerol-3-phosphate dehydrogenase (*GPD1* and *GPD2*) were constructed based on the SR8A5 strain. We reasoned that reduced glycerol production might lead to more acetate reduction. While we can eliminate glycerol production by deleting both *GPD1* and *GPD2*, the resulting mutant can be extremely sick (Guadalupe Medina et al. 2010).Therefore, we undertook approaches to partially abolish Gpd activity through truncations of the promoter or coding regions. 60 bp and 80 bp upstream promoter regions from the start codon of *GPD1* were deleted in the SR8A5-1 and SR8A5-2 strains, respectively. Additionally, the coding region of *GPD2* was deleted in the SR8A5-1 and SR8A5-2 strains, generating the SR8A5-3 and SR8A5-4 strains, respectively (Ding et al. 2013).

We performed fermentation experiments by the engineered strains using a mixture of glucose,

xylose and acetate under anaerobic conditions. As shown in Figure S3, although the genetic perturbations led to reduced glycerol production, the consumed amounts of acetate by the SR8A5-1, SR8A5-2, and SR8A5-3 were almost identical to their parental strain (SR8A5). The SR8A5-4 strain consumed even less acetate because of the impaired growth and sugar consumption caused by the major loss of Gpd activity. We performed another fermentation experiments by the engineered strains with impaired glycerol production using a mixture of glucose and acetate under anaerobic conditions. None of the engineered strain was able to consumed acetate during the glucose fermentation. Overall, these experiments demonstrated that increasing NADH levels by altered glycerol-3-phosphate dehydrogenase expression levels couldn't improve acetate reduction and the surplus NADH generated during the xylose fermentation under anaerobic conditions might be sufficient to sustain the acetate reduction pathway in our engineered yeast strains.

3.5. Improved fermentation of a lignocellulosic hydrolysate by the engineered SR8A6S3 strain

Dilute acid pre-treatment of lignocellulosic biomass generates a solid fraction containing cellulose and lignin and a liquid fraction containing glucose, xylose, and acetate. Typically, the liquid fraction contains 20 g/L glucose, 50 g/L xylose, and 10 g/L acetate. We performed a fermentation experiment using a liquid fraction obtained from dilute acid pretreated *Miscanthus* and our optimized yeast strain (SR8A6S3). As shown in Figure 5, both the control strain (SR8) and engineered SR8A6S3 strain depleted glucose within 12 hours. While the SR8A6S3 strain was able to deplete xylose within 48 hours along with the co-consumption with 4.11 g/L acetate, the SR8 strain finished xylose fermentation at 60 hours without consuming acetate at all. As a result, the ethanol yield of the SR8A6S3 strain increased 18.4% (0.395 vs. 0.468 g ethanol/g sugars) as compared to that of the SR8 strain. This substantial yield increase is due to not only from the consumed acetate, but also from the reduced byproduct formation. The glycerol and xylitol yield of the SR8A6S3 strain decreased by 40.3% (0.073 vs. 0.033g glycerol/g sugars, 0.112 vs. 0.078 g xylitol/g xylose) as compare to that of the SR8 strain

(Table 4).

4. Discussion

Improving the xylose fermentation ability of *S. cerevisiae* yeast has been researched extensively. Engineered *S. cerevisiae* strains with XR-XDH pathway showed low ethanol yields and high byproduct yields because of the redox imbalance caused by the cofactor difference of XR and XDH. Therefore, metabolic engineering strategies to improve xylose fermentation by engineered yeast with XR and XDH were attempted by balancing the redox through modifying cofactor preferences of XR and XDH, or by providing an appropriate electron acceptor for re-oxidizing surplus NADH under anaerobic conditions. The cofactor preferences of XR or XDH have been successfully altered by protein engineering (Watanabe et al. 2005; Watanabe et al. 2007) and mutated XR and XDH were shown to be effective to some extent for reducing xylitol accumulation as well as increasing the ethanol yield from xylose. Also, the supplementation of electron acceptors, such as furfural, 5-hydroxymethyl furfural, acetoin into fermentation media led to improved xylose fermentation (Verho et al. 2003; Wahlbom and Hahn-Hagerdal 2002; Zhang et al. 2012). However, these strategies came along with 'collateral damage'. Either impaired cell growth or reduced enzyme activity have been observed unintendedly. Engineered *S. cerevisiae* with the XI pathway can bypass the redox imbalance problem as cofactors are not necessary for XI. As a result, the ethanol yields by XI strains were higher than those by the engineered yeast with XR-XDH.

However, if acetate, a major fermentation inhibitor present in lignocellulosic hydrolysates, were to serve as a redox sink and is converted into less inhibitory products, both the cofactor imbalance problems and the toxicity of acetate can be alleviated or even eliminated. In addition, the reduced acetate would contribute to the final ethanol titer. In the previous study, Na Wei et al. have demonstrated the beneficial effects resulted from acetate and xylose co-consumition by the engineered strain, whereas the consumed acetate was marginal and the performance of the engineered strain in

actual lignocellulosic hydrolysate was not shown (Na Wei et al. 2013). In this study, as much more acetate (~ 3.5 fold as compare to previous number) was co-consumed with xylose, the ethanol yield of the SR8A6S3 strain reached up to 0.446 g/g sugars in terms of YP fermentation and 0.468 g/g sugars in terms of lignocellulosic hydrolysate fermentation, which is comparable or better to the best engineered yeast with XI so far (Zhou et al. 2012). This *in situ* detoxification strategy of coupling the oxidoreductive xylose metabolism and acetate reduction pathway shows great potential towards the industrial production of ethanol from lignocellulosic feedstock.

There are three major factors which might limit the metabolic fluxes of the acetate reduction pathway. These include the activities of key enzymes (ACS and AADH), intracellular ATP levels and NADH levels (Figure 1). This study investigated these possible limiting factors using relevant genetic and environmental perturbations and concluded that the major limiting factor of the acetate reduction pathway in yeast might be the activities of key enzymes (AADH and ACS) rather than the NADH or ATP levels. In order to increase the activities of AADH and ACS, we first decided to use a codon-optimized *adhE* because the strain SR8A2 expressing *E. coli adhE* under the control of a strong constitutive yeast promoter barely consumed acetate. As expected, simple codon-optimization of *E. coli adhE* based on a previous report (Wiedemann and Boles 2008) resulted in dramatically increased AADH activity. Moreover, we constructed two more strains exhibiting increasing activities of AADH by introducing two, and three copies of the codon optimized *adhE*. When we investigated the relationship between AADH activities and the amounts of acetate consumption by the three strains, we observed that higher AADH activities result in more acetate consumption, but there is a saturation after introducing three copies of the codon-optimized *adhE*. We reasoned that ACS activity might also be limiting because acetyl-CoA production in the cytosol of yeast has been discussed as limiting step for the production of acetyl-CoA-derived metabolites in previous reports (Lian et al. 2014; Shiba et al. 2007). Initially, we overexpressed endogenous *ACS1* and *ACS2* in the SR8A6 strain, but the acetate consumption capacity by the resulting yeast did not change (data not shown), which is consistent with

the previous finding that yeast Acs might be post-translationally regulated (Shiba et al. 2007). Therefore, we chose to overexpress a mutant *ACS* from *Salmonella enterica* ($SeAcs^{L641P}$) which is reported to work better for the production of acetyl-CoA-derived products (Kildegaard et al. 2016; Lian et al. 2014). Genomic integration of three copies of the mutant *Salmonella enterica ACS* into the SR8A5 strain resulted in the SR8A6S3 strain. As a result, the ACS activity in the SR8A6S3 was two-fold higher than that in the SR8A6 strain. The SR8A6S3 consumed 34.5% more acetate, produced 8.51% more ethanol and 34.3% less reduced byproducts (glycerol and xylitol) than the SR8A6 strain. This result suggests that ACS activity also plays a significant role in the acetate reduction pathway.

As glucose is the most favorable carbon source for yeast, the intraocular ATP levels can be maintained well under glucose fermentation. As such, glucose pulse-feeding to continuously generate ATP has been implemented in previous studies (Friis et al. 2009; Pedler et al. 1997). In order to boost metabolic fluxes in the acetate reduction pathway, enough ATP needs to be supplied throughout the fermentation because the ACS reaction uses 2 ATP equivalents for producing acetyl-CoA from acetate. We hypothesized that better ATP supply from glucose pulse-feeding might improve acetate consumption. However, we failed to observe any improvements in acetate consumption from the pulse-feeding experiment (Figure S2). Our results from the pulse-feeding experiment for continuous ATP supply and the promoter truncation of *GPD1* to increase intracellular NADH levels suggest that ATP and NADH levels in our engineered yeast might not be severe limiting factors (Figure S3).

While the final engineered strain SR8A6S3 showed decent improvement in lignocellulosic hydrolysate fermentation as compared to the control strain (SR8), the extent of the improvement was not as significant as that observed in the YP medium fermentation (Table 4). These results indicate that there might be other limiting factors in the lignocellulosic hydrolysate fermentation. For instance, well-known fermentation inhibitors, such as 5-hydroxymethylfurfural (HMF), furfural might hinder the overall sugar metabolism of our engineered strain. Besides, furfural and HMF could serve as a redox sink and thus compete for surplus NADH with the acetate reduction pathway.

Through the optimization of the acetate reduction pathway in engineered yeast, we were able to substantially improve the ethanol yield from xylose as well as to detoxify acetate during the mixed sugar fermentation in the presence of acetate. We identified that the key enzyme activity rather than ATP and NADH levels might be the major limiting factor of the acetate reduction pathway in our engineered yeast. The ethanol yield (0.463 g/g xylose) obtained from the lignocellulosic hydrolysate fermentation by the optimized engineered strain (SR8A6S3) is so far the highest among other engineered strains with XR-XDH pathway, and is comparable to the best engineered strain with XI pathway.

Acknowledgements

This work was supported by funding from the Energy Biosciences Institute and the Research Initiative Program of KRIBB. The pretreated *Miscanthus* hydrolysate was provided by National Renewable Energy Lab (NREL). TLT was supported by the Agriculture and Food Research Initiative Competitive Grant No. 2015-67011-22806 from the USDA National Institute of Food and Agriculture. The authors declare that they have no conflict of interest

References

Atteia A, van Lis R, Mendoza-Hernandez G, Henze K, Martin W, Riveros-Rosas H, Gonzalez-Halphen D. 2003. Bifunctional aldehyde/alcohol dehydrogenase (ADHE) in chlorophyte algal mitochondria. Plant Mol Biol 53(1-2):175-88.

Axe DD, Bailey JE. 1995. Transport of lactate and acetate through the energized cytoplasmic membrane of *Escherichia coli*. Biotechnol Bioeng 47(1):8-19.

Burtner CR, Murakami CJ, Kennedy BK, Kaeberlein M. 2009. A molecular mechanism of chronological aging in yeast. Cell Cycle 8(8):1256-70.

Chen Y, Stabryla L, Wei N. 2016. Improved Acetic Acid Resistance in *Saccharomyces cerevisiae* by Overexpression of the *WHI2* Gene Identified through Inverse Metabolic Engineering. Appl Environ Microbiol 82(7):2156-66.

DiCarlo JE, Norville JE, Mali P, Rios X, Aach J, Church GM. 2013. Genome engineering in *Saccharomyces cerevisiae* using CRISPR-Cas systems. Nucleic Acids Res 41(7):4336-43.

Ding WT, Zhang GC, Liu JJ. 2013. 3' Truncation of the *GPD1* promoter in *Saccharomyces cerevisiae* for improved ethanol yield and productivity. Appl Environ Microbiol 79(10):3273-81.

Fontaine L, Meynial-Salles I, Girbal L, Yang X, Croux C, Soucaille P. 2002. Molecular characterization and transcriptional analysis of *adhE2*, the gene encoding the NADH-dependent aldehyde/alcohol dehydrogenase responsible for butanol production in alcohologenic cultures of *Clostridium acetobutylicum* ATCC 824. J Bacteriol 184(3):821-30.

Friis RM, Wu BP, Reinke SN, Hockman DJ, Sykes BD, Schultz MC. 2009. A glycolytic burst drives glucose induction of global histone acetylation by picNuA4 and SAGA. Nucleic Acids Res 37(12):3969-80.

Gietz RD, Sugino A. 1988. New yeast-*Escherichia coli* shuttle vectors constructed with in vitro mutagenized yeast genes lacking six-base pair restriction sites. Gene 74(2):527-34.

Guadalupe Medina V, Almering MJ, van Maris AJ, Pronk JT. 2010. Elimination of glycerol production

in anaerobic cultures of a *Saccharomyces cerevisiae* strain engineered to use acetic acid as an electron acceptor. Appl Environ Microbiol 76(1):190-5.

Haitani Y, Tanaka K, Yamamoto M, Nakamura T, Ando A, Ogawa J, Shima J. 2012. Identification of an acetate-tolerant strain of *Saccharomyces cerevisiae* and characterization by gene expression analysis. J Biosci Bioeng 114(6):648-51.

Ho NW, Chen Z, Brainard AP. 1998. Genetically engineered *Saccharomyces* yeast capable of effective cofermentation of glucose and xylose. Appl Environ Microbiol 64(5):1852-9.

Jeffries TW, Jin YS. 2004. Metabolic engineering for improved fermentation of pentoses by yeasts. Appl Microbiol Biotechnol 63(5):495-509.

Jonsson LJ, Alriksson B, Nilvebrant NO. 2013. Bioconversion of lignocellulose: inhibitors and detoxification. Biotechnol Biofuels 6(1):16.

Karhumaa K, Garcia Sanchez R, Hahn-Hagerdal B, Gorwa-Grauslund MF. 2007. Comparison of the xylose reductase-xylitol dehydrogenase and the xylose isomerase pathways for xylose fermentation by recombinant *Saccharomyces cerevisiae*. Microb Cell Fact 6:5.

Kawahata M, Masaki K, Fujii T, Iefuji H. 2006. Yeast genes involved in response to lactic acid and acetic acid: acidic conditions caused by the organic acids in *Saccharomyces cerevisiae* cultures induce expression of intracellular metal metabolism genes regulated by Aft1p. FEMS Yeast Res 6(6):924-36.

Kildegaard KR, Jensen NB, Schneider K, Czarnotta E, Ozdemir E, Klein T, Maury J, Ebert BE, Christensen HB, Chen Y and others. 2016. Engineering and systems-level analysis of *Saccharomyces cerevisiae* for production of 3-hydroxypropionic acid via malonyl-CoA reductase-dependent pathway. Microb Cell Fact 15(1):53.

Kim SR, Skerker JM, Kang W, Lesmana A, Wei N, Arkin AP, Jin YS. 2013. Rational and evolutionary engineering approaches uncover a small set of genetic changes efficient for rapid xylose fermentation in *Saccharomyces cerevisiae*. PLoS One 8(2):e57048.

Klinke HB, Thomsen AB, Ahring BK. 2004. Inhibition of ethanol-producing yeast and bacteria by degradation products produced during pre-treatment of biomass. Appl Microbiol Biotechnol 66(1):10-26.

Kuyper M, Hartog MM, Toirkens MJ, Almering MJ, Winkler AA, van Dijken JP, Pronk JT. 2005. Metabolic engineering of a xylose-isomerase-expressing *Saccharomyces cerevisiae* strain for rapid anaerobic xylose fermentation. FEMS Yeast Res 5(4-5):399-409.

Li X, Park A, Estrela R, Kim S-R, Jin Y-S, Cate JHD. 2016. Comparison of xylose fermentation by two high-performance engineered strains of *Saccharomyces cerevisiae*. Biotechnology Reports 9:53-56.

Lian J, Si T, Nair NU, Zhao H. 2014. Design and construction of acetyl-CoA overproducing *Saccharomyces cerevisiae* strains. Metab Eng 24:139-49.

Palmqvist E, Hahn-Hägerdal B. 2000a. Fermentation of lignocellulosic hydrolysates. I: inhibition and detoxification. Bioresource Technology 74(1):17-24.

Palmqvist E, Hahn-Hägerdal B. 2000b. Fermentation of lignocellulosic hydrolysates. II: inhibitors and mechanisms of inhibition. Bioresource Technology 74(1):25-33.

Parekh RN, Shaw MR, Wittrup KD. 1996. An integrating vector for tunable, high copy, stable integration into the dispersed Ty delta sites of *Saccharomyces cerevisiae*. Biotechnol Prog 12(1):16-21.

Pedler SM, Wallace PG, Wallace JC, Berry MN. 1997. The fate of glucose in strains S288C and S173-6B of the yeast *Saccharomyces cerevisiae*. Yeast 13(2):119-25.

Shiba Y, Paradise EM, Kirby J, Ro DK, Keasling JD. 2007. Engineering of the pyruvate dehydrogenase bypass in *Saccharomyces cerevisiae* for high-level production of isoprenoids. Metab Eng 9(2):160-8.

Tanaka K, Ishii Y, Ogawa J, Shima J. 2012. Enhancement of acetic acid tolerance in *Saccharomyces cerevisiae* by overexpression of the *HAA1* gene, encoding a transcriptional activator. Appl

Environ Microbiol 78(22):8161-3.

van den Berg MA, de Jong-Gubbels P, Kortland CJ, van Dijken JP, Pronk JT, Steensma HY. 1996. The two acetyl-coenzyme A synthetases of *Saccharomyces cerevisiae* differ with respect to kinetic properties and transcriptional regulation. J Biol Chem 271(46):28953-9.

Verho R, Londesborough J, Penttila M, Richard P. 2003. Engineering redox cofactor regeneration for improved pentose fermentation in *Saccharomyces cerevisiae*. Appl Environ Microbiol 69(10):5892-7.

Vickers CE, Bydder SF, Zhou Y, Nielsen LK. 2013. Dual gene expression cassette vectors with antibiotic selection markers for engineering in *Saccharomyces cerevisiae*. Microb Cell Fact 12:96.

Wahlbom CF, Hahn-Hagerdal B. 2002. Furfural, 5-hydroxymethyl furfural, and acetoin act as external electron acceptors during anaerobic fermentation of xylose in recombinant *Saccharomyces cerevisiae*. Biotechnol Bioeng 78(2):172-8.

Wang CH, Labbe RF, Christensen BE, Cheldelin VH. 1952. Utilization of C14 labeled pyruvate and acetate by yeast. J Biol Chem 197(2):645-53.

Watanabe S, Kodaki T, Makino K. 2005. Complete reversal of coenzyme specificity of xylitol dehydrogenase and increase of thermostability by the introduction of structural zinc. J Biol Chem 280(11):10340-9.

Watanabe S, Pack SP, Saleh AA, Annaluru N, Kodaki T, Makino K. 2007. The positive effect of the decreased NADPH-preferring activity of xylose reductase from *Pichia stipitis* on ethanol production using xylose-fermenting recombinant *Saccharomyces cerevisiae*. Biosci Biotechnol Biochem 71(5):1365-9.

Wei N, Oh EJ, Million G, Cate JH, Jin YS. 2015. Simultaneous utilization of cellobiose, xylose, and acetic acid from lignocellulosic biomass for biofuel production by an engineered yeast platform. ACS Synth Biol 4(6):707-13.

Wei N, Quarterman J, Kim SR, Cate JH, Jin YS. 2013. Enhanced biofuel production through coupled acetic acid and xylose consumption by engineered yeast. Nat Commun 4:2580.

Wiedemann B, Boles E. 2008. Codon-optimized bacterial genes improve L-Arabinose fermentation in recombinant *Saccharomyces cerevisiae*. Appl Environ Microbiol 74(7):2043-50.

Zhang GC, Kong, II, Kim H, Liu JJ, Cate JH, Jin YS. 2014. Construction of a quadruple auxotrophic mutant of an industrial polyploid *Saccharomyces cerevisiae* strain by using RNA-guided Cas9 nuclease. Appl Environ Microbiol 80(24):7694-701.

Zhang GC, Liu JJ, Ding WT. 2012. Decreased xylitol formation during xylose fermentation in *Saccharomyces cerevisiae* due to overexpression of water-forming NADH oxidase. Appl Environ Microbiol 78(4):1081-6.

Zhang GC, Liu JJ, Kong, II, Kwak S, Jin YS. 2015. Combining C6 and C5 sugar metabolism for enhancing microbial bioconversion. Curr Opin Chem Biol 29:49-57.

Zhou H, Cheng JS, Wang BL, Fink GR, Stephanopoulos G. 2012. Xylose isomerase overexpression along with engineering of the pentose phosphate pathway and evolutionary engineering enable rapid xylose utilization and ethanol production by *Saccharomyces cerevisiae*. Metab Eng 14(6):611-22.

Figure legends

Fig. 1 Illustration of the xylose and acetate co-consumption pathway in engineered *S. cerevisiae.* ACS*, AADH, XR and XDH stand for mutant acetyl-CoA synthetase from *Salmonella enterica*, acetylating acetaldehyde dehydrogenase from *E. coli*, xylose reductase, and xylitol dehydrogenase from *Scheffersomyces stipitis*, respectively. The most likely rate-limiting factors (ACS*, AADH, ATP, and NADH) for acetate consumption are in bold.

Fig. 2 Enzyme activities of AADH (A) and ACS (B) in the series of engineered *S. cerevisiae* strains. *WTadhE* denotes the wild type AADH, *COadhE* denotes the codon-optimized AADH, *ACS** denotes the mutant ACS ($SeAcs^{L641p}$) from *Salmonella enterica*. Numbers following the gene names stand for copy numbers of each gene expression cassette introduced into parental strain SR8. Data are presented as mean value and standard deviation of three independent biological replicates.

Fig. 3 Consumed acetate (A), ethanol yield (B), xylitol yield (C), glycerol yield (D) of the engineered strains were evaluated at the end of the fermentation in YP medium containing 20 g/L glucose, 80 g/L xylose and 8 g/L of acetate (96 h). Data are presented as mean value and standard deviation of three independent biological replicates.

Fig. 4 Fermentation performances of a control strain SR8 (A) and the SR8A6S3 strain (B) were evaluated in YP medium containing 20g /L of glucose, 80 g/L xylose and 8 g/L acetate. Data are presented as mean value and standard deviation of three independent biological replicates.

Fig. 5 Fermentation performance of a control strain SR8 (A) and the SR8A6S3 (B) stains were evaluated in a lignocellulosic hydrolysate liquid fraction. Data are presented as mean value and standard deviation of three independent biological replicates.

Table. 1 Important primers used in this study

Primers	sequence
H1-U/H1-D	gggcccgcatgcgaattcctatcagcttttttttgcgc/gggcccgcatgcggtaccccagaatatcttggtgaagc
H2-U/H2-D	gggcccgcatgcgagagcaatcaatgcaatgg/gggcccgcatgcaagcttggttgttctcaaccttctac
pPGK1-U	gggcccgcatgcgcatgcaagaaattaccgtcgctcgt
pPGK1-D	gggcccgcatgcgtcgacagacattgttttatatttgt
tPGK1-U	gggcccgcatgcggatcctaaattgaattgaattgaaa
tPGK1-D	gggcccgcatgcccatgggacttttttttgttgcaagtg
adhE-U	gggcccgcatgcgtcgacgcatgcaagaaattaccgtcgctcgt
adhE-D	gggcccgcatgcggatccccatgggacttttttttgttgcaagtg
adhEdonor-U	atgactgctcaacaaggtgtaccaataaagataaccaataaggagattgctcaagaattcgaagaaattaccgtcgctcg
adhEdonor-D	gatcagttgtttgcccaattgcttcaaaaggtttagaatttccagggtgtatggtaatgcgttgcaagtgggatgagctt

Table. 2 Important plasmids used in this study

Plasmids	Resource
YIplac211	(Gietz and Sugino 1988)
pITy3	(Parekh et al. 1996)
YIplac211-H1H2	This study
pITy3-pPGK1-WTadhE-tPGK1	This study
pITy3-pPGK1-COadhE-tPGK1	This study
YIplac211-H1H2-WTadhE	This study
YIplac211-H1H2-COadhE	This study
gRNA-pho13-G418	This study
ACS*Opt	(Lian et al. 2014)
Cas9-NAT	(Zhang et al. 2014)

Table. 3 Strains used in this study

Strains	Description	References
SR8	Efficient xylose-utilizing strain engineered from strain D452-2	(Kim et al. 2013)
SR8A2	SR8 expressing one copy of WTadhE overexpression cassette	This study
SR8A4	SR8 expressing one copy of COadhE overexpression cassette	This study
SR8A5	SR8 expressing two copies of COadhE overexpression cassette	This study
SR8A5-Cas9	SR8A5 containing plasmid Cas9-NAT	This study
SR8A6	SR8 expressing three copies of COadhE overexpression cassette	This study
SR8A6S3	SR8A6 expressing three copies of mutant Salmonella *ACS* gene overexpression cassette	This study
SR8A5-1	*GPD1* gene promoter region -60 bp truncation in SR8A5	This study
SR8A5-2	*GPD1* gene promoter region -80 bp truncation in SR8A5	This study
SR8A5-3	*GPD2* gene deletion in strain SR8A5-1	This study
SR8A5-4	*GPD2* gene deletion in strain SR8A5-2	This study

Table 4 Fermentation properties of SR8 and SR8A6S3 in hydrolysate condition

Conditions	Strains	*P**ethanol (g/h)	*Y**ethanol (g/g consumed sugar)	*Y**xylitol (g/g consumed xylose)	*Y**glycerol (g/g consumed sugar)	Consumed acetate (g/L)
Hydrolysate OD 10 inoculum	SR8	0.566±0.02	0.395±0.01	$(11.20\pm0.07)*10^{-2}$	$(7.30\pm0.11)*10^{-2}$	0.69±0.01
	SR8A6S3	0.733±0.01	0.468±0.006	$(7.80\pm0.05)*10^{-2}$	$(3.25\pm0.08)*10^{-2}$	4.11±0.03
YP OD 1 inoculum	SR8	0.36±0.02	0.344±0.011	$(8.50\pm0.25)*10^{-2}$	$(8.87\pm0.33)*10^{-2}$	0.31±0.13
	SR8A6S3	0.49±0.02	0.446±0.003	$(2.40\pm0.09)*10^{-2}$	$(2.68\pm0.21)*10^{-2}$	7.1±0.22

*: *P* stands for Productivity; *Y* strands for yield.

Results are presented as the mean value and standard deviation of three independent biological replicate.

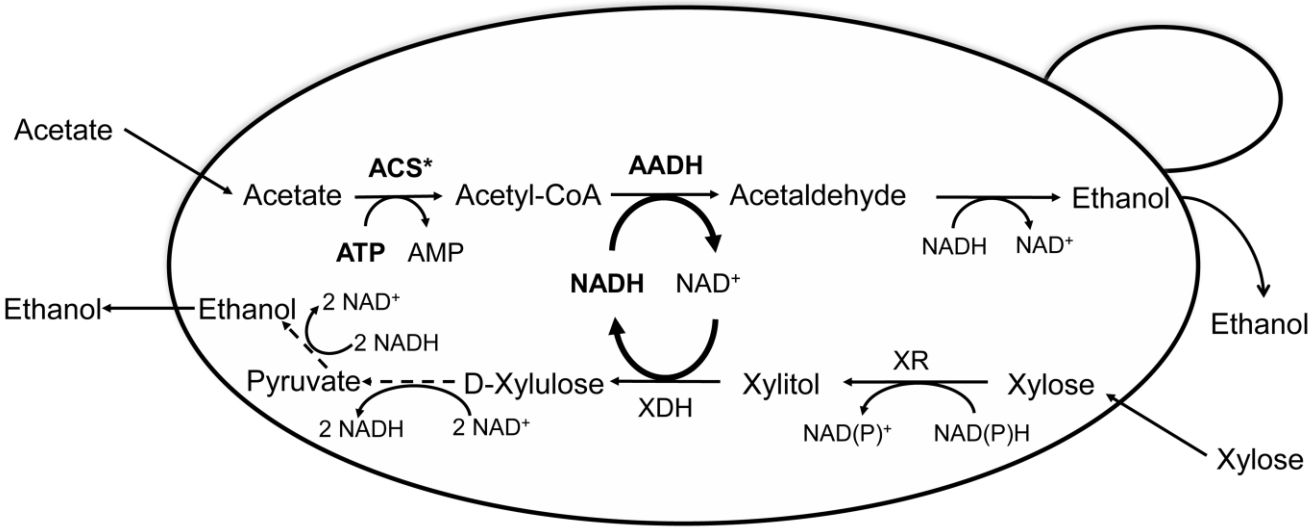

Figure 1

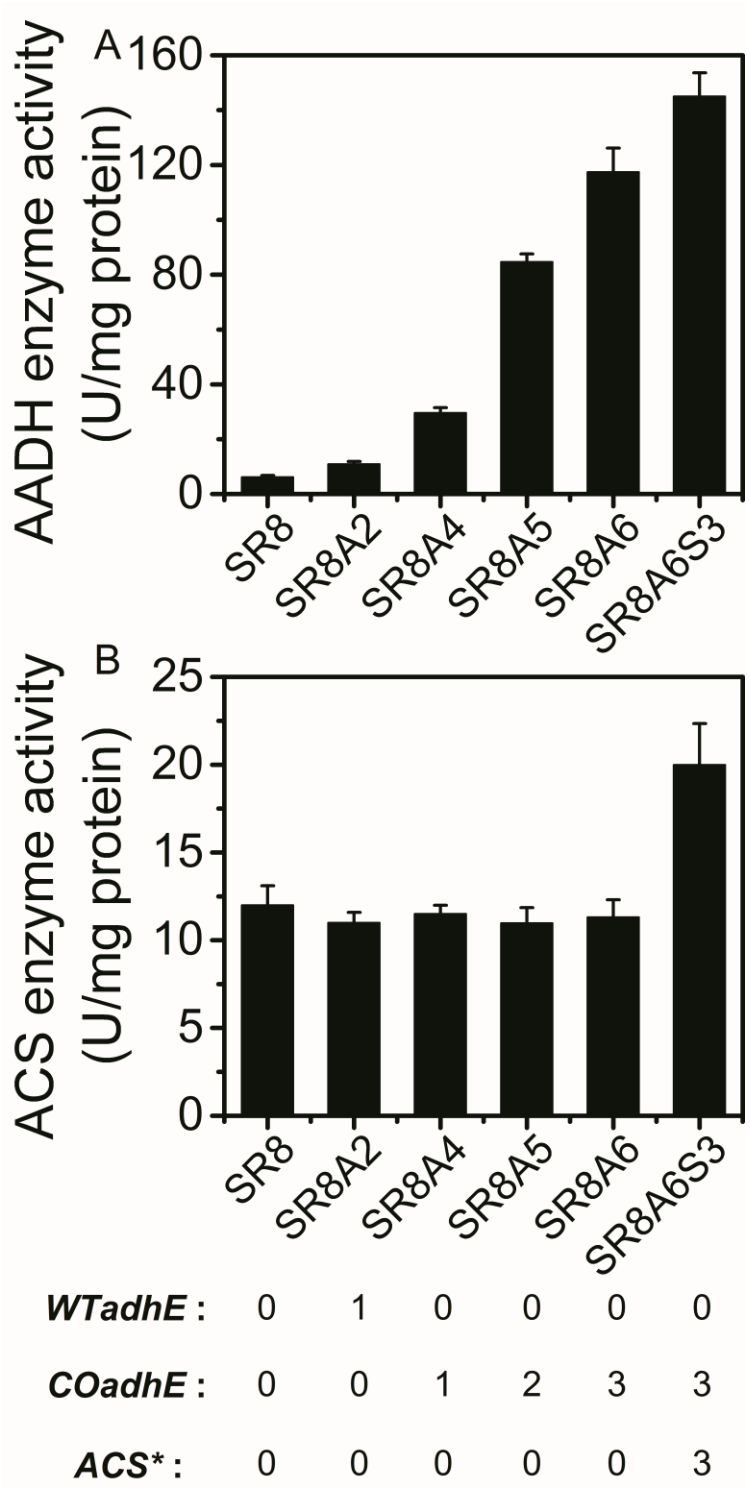

Figure 2

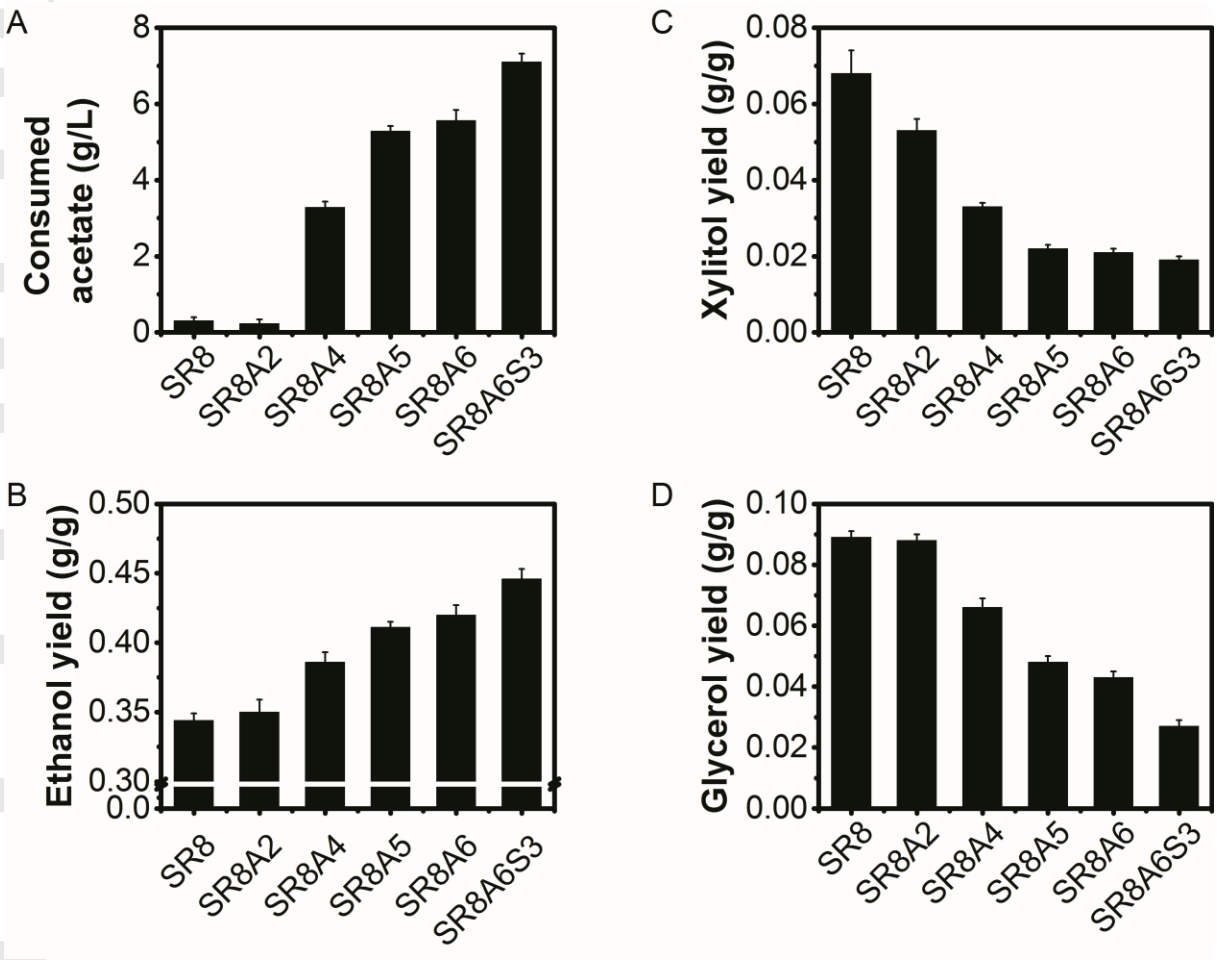

Figure 3

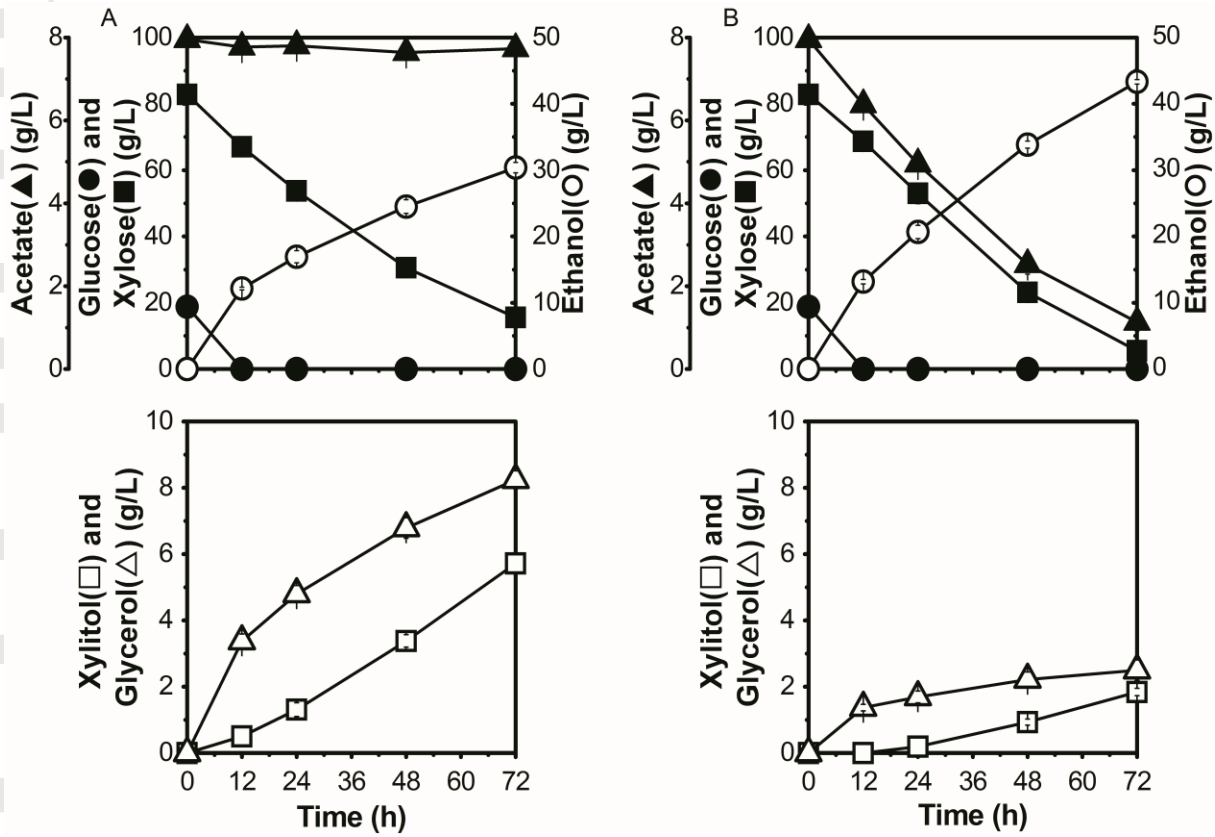

Figure 4

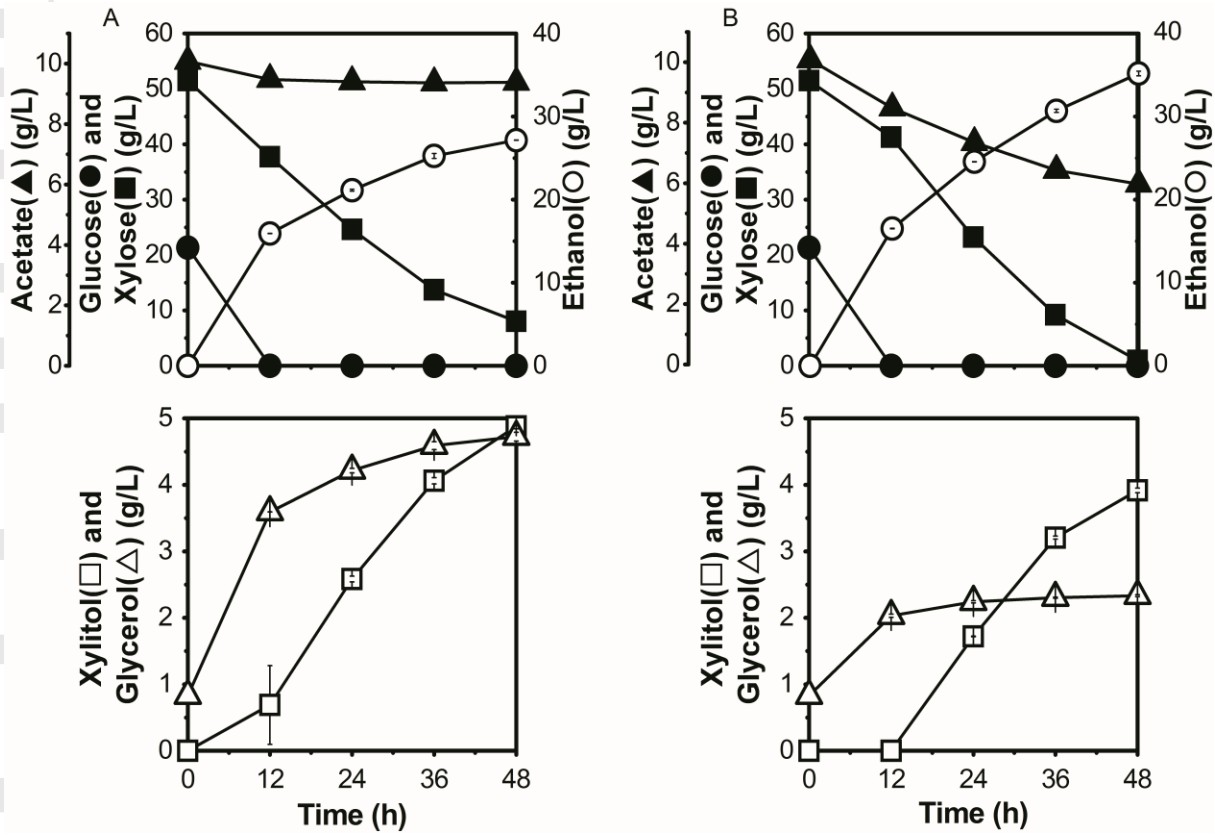

Figure 5